Rev. Adv. Mater. Sci. 33 (2013) 51-55

STUDY ON SURFACE MODIFICATION OF NANOCRYSTALLINE COPPER BY Ti IONS IMPLANTATION

Wan Ming Lin, Yu Shui Qian, Ying Hui Wei and Li Feng Hou

College of Materials Science and Engineering of Taiyuan University of Technology, Taiyuan Shanxi 030024,China

Received: October 17, 2011

Abstract. The combination of surface modification and nanotechnology was applied to modify the surface properties of metal materials. Titanium ions were implanted into the surface nanocrystalline copper by using metal vapor vacuum arc (MEVVA). Titanium implantation was carried out at the chosen ion doses 2×10^{17} ions/cm^2 and the energy of 40 keV. The surface microstructure and concentration distribution of implanted ions were characterized by using transmission electron microscope (TEM), X-ray diffractometer (XRD), Auger electron spectroscopy (AES). The results showed that after the surface mechanical attrition treatment (SMAT) the microstructure of the surface layer may be refined into the nanoscale. The concentration of implanted ions followed Gauss distribution. The specimens after ion implantation have a remarkable enhancement of corrosion resistance with respect to the specimens without the surface treatment.

1. INTRODUCTION

Surface nanocrystallization (SNC) is a novel method for improving materials properties [1]. It has been demonstrated that among the different techniques used to produce nanostructured layers, surface mechanical attrition treatment (SMAT), accomplished by surface shot peening, is an effective way of creating localized plastic deformation resulting in grain refinement down to the nanometer scale without changing the chemical composition of the material [2]. The SMAT process has been successfully applied to many material systems including aluminum [3], iron [4], stainless steel [5] and titanium [6,7].However, SMATed alloys also suffer from low resistance to corrosion, which limit their applications [8,9]. Surface modification has been found to be an efficient way to improve the corrosion properties of metallic materials without changing the substrate properties [10].

The ion implantation technique as a surface treatment has been used to enhance physical and chemical performances of metals [11-14]. The result of ion implantation into materials is the formation of a near-surface alloy of graded composition that has no well defined interface with respect to the substrate, in contrast to a deposition layer. A graded alloy can be produced from the surface to the unchanged underlying bulk alloy so that both the surface and the bulk can be independently optimized [15].

Titanium (Ti) is a good candidate as a corrosion resistant material due to protective oxide films on titanium usually formed when the metal is present in moisture. In the work, the combination of surface modification and nanotechnology was applied to modify the surface properties of metal materials. Ti ion implantation into the SMATed copper was performed by using an ion implantation machine with a MEVVA ion source. The objective of this study is

Corresponding author: Wan Ming Lin, e-mail: linwm1970@126.com

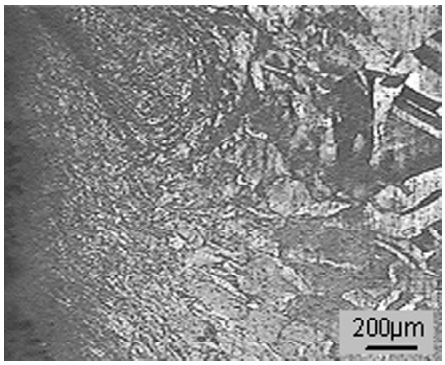

Fig. 1. Microscopic cross-sectional observation of pure copper after the SMAT for 60 min.

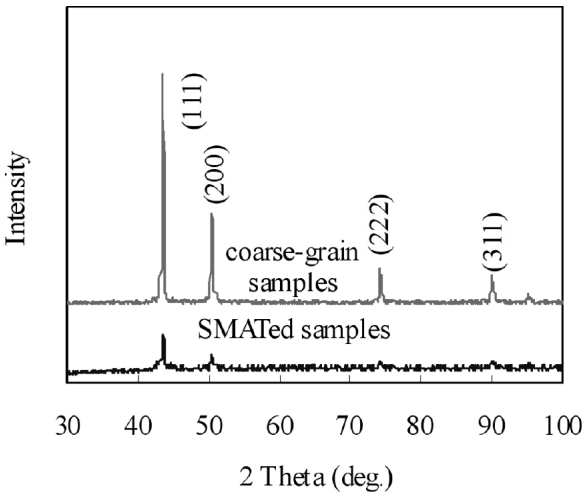

Fig. 2. X-ray diffraction patterns from the coarse-grain samples and the SMATed samples.

to improve the corrosion resistance of the SMATed copper by implantation of Ti ions.

2. MATERIAL AND METHODS

Before treatment, the Copper plate (100×100×6 mm) was annealed for 2 h at 923K under vacuum to eliminate the effect of mechanical polishing on the surface and to obtain homogeneously coarse grains. The copper plate was subjected to surface mechanical attrition treatment (SMAT) process as follows. GCr15 balls with diameter 8 mm were placed in a chamber vibrated by a generator, then the balls were resonated and impacted the sample surface to be treated at the upper side of the chamber [16]. The sample was treated for 60 min under vacuum at room temperature with vibration frequency 50 Hz.

Ti ion implantation was performed by using an ion implantation machine with a MEVVA ion source. Ti ions were implanted into one side of the plates with an acceleration energy of 40 keV and ion-beam current of 2 mA. The implantation dose was set at 2×10^{17} ions/cm^2 . The vacuum in the target chamber was kept at 1×10^{-4} Pa.

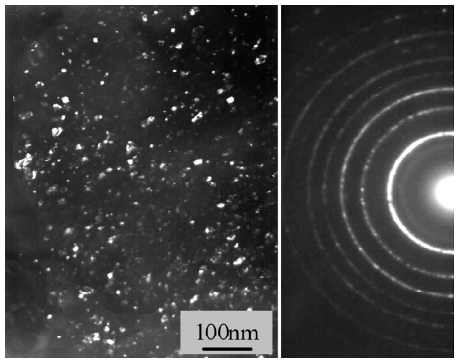

Fig. 3. Bright-field TEM images and the corresponding selected area electron diffraction (SAED) pattern of the top surface layer of the SMATed sample.

The corrosion behavior of the samples was determined by potentiodynamic anodic polarization tests (PS-168A). The specimen with exposed area of 10×10 mm^2 served as a working electrode. A platinum electrode was used as the reference electrode. Prior to the measurement, the samples were exposed to the test solution and stabilized for 10 min. The electrolyte was 0.1 mol/L$CuSO_4$ +0.05 mol/LH_2SO_4 solution prepared by using reagent grade chemicals dissolved in distilled water.

3. RESULTS AND DISCUSSION

3.1. Surface nanocrystallization of pure copper

Fig. 1 shows an optical microscope image of the cross-sectional morphology of the SMATed copper specimen. It is apparent that the grain size varies through the thickness of the specimen. The finest grains occur in the surface layer, from the surface to about 200 μm depth, where grain boundaries could

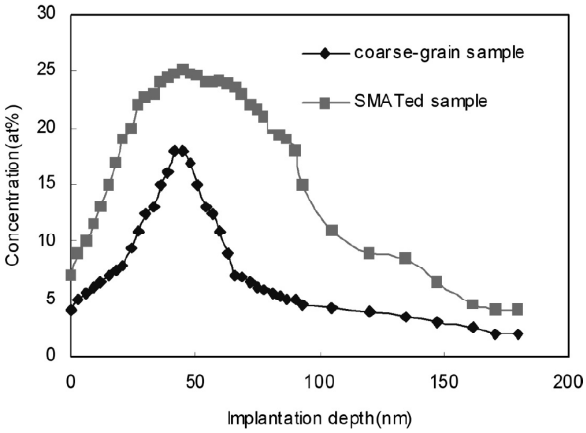

Fig. 4. Ti concentration profiles of the SMATed sample and coarse-grain sample along the depth by using AES for pure copper.

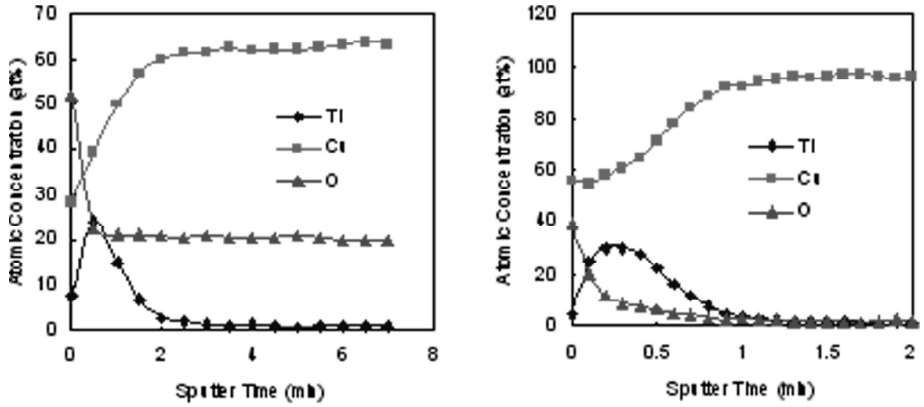

Fig. 5. Influence of sputter time on atomic concentration: (a) coarse-grain samples, (b) SMATed samples.

not be clearly identified due to severe plastic deformation. It is noteworthy that the thickness of the surface deformation layer of the Cu plate was not uniform along the depth, indicating heterogeneity of plastic deformation induced by the repeated peening. XRD patterns of top surface layer of samples before and after the SMAT treatments are shown in Fig. 2. There is evident broadening of Bragg reflection profiles, which can be attributed to the crystalline imperfection induced by small grain size and microstrain. After the SMAT treatment for 60 min, the average grain size in the top surface layer was found to be about 28 nm. The nanocrystalline grains were mostly equi-axed with random crystallographic orientations indicated by SAED patterns (Fig. 3).

There was a transition layer, about 200 μm thick, between the nanocrystalline layer and the matrix, where the grain size was sub-micrometer scale. The microstructure in this layer had characteristics of both the surface layer and the matrix, which was attributed to plastic deformation to a lesser extent.

3.2. Ion implantation

Fig. 4 shows the atomic concentration distribution of Ti in the SMAT sample and the coarse-grained sample along the depth by using AES for pure copper. Influence of sputter time on the atomic concentration distribution shown in Fig. 5.

The titanium implantation in the coarse-grained sample penetrates about 70 nm with a Gaussian distribution and exhibits a maximum at a depth of 45 nm. In the SMAT sample, the maximum penetration depth is 160 nm with a maximum concentration located at about 45 nm beneath the surface.

Because it is a non-equilibrium process, the formation of alloy on the surface during ion implantation is not affected by phase equilibrium or solid solution. Hence, in general, all elements can be implanted in each other. In addition to the defects on the surface of the copper substrate due to “irradiation damage” during ion implantation, the numerous high density defects (vacancies) arising from plastic deformation in the SMAT process facilitated diffusion of Ti atoms.

Nanocrystalline materials are structurally characterized by ultra-fine grains and a large number of grain boundaries (GBs), with numerous vacancies whose energy of formation is very low. Moreover, the density of vacancies and their migration rate are higher in grain boundaries because the atoms at grain boundaries are disordered and lattice distortion is more severe than in the interior of a grain. As a result, these defective GBs (especially the numerous triple junctions), acting as “short circuit” diffusion channels, allow Ti atoms to more easily diffuse to the surface in nanocrystalline materials than in their coarse-grained polycrystalline counterparts.

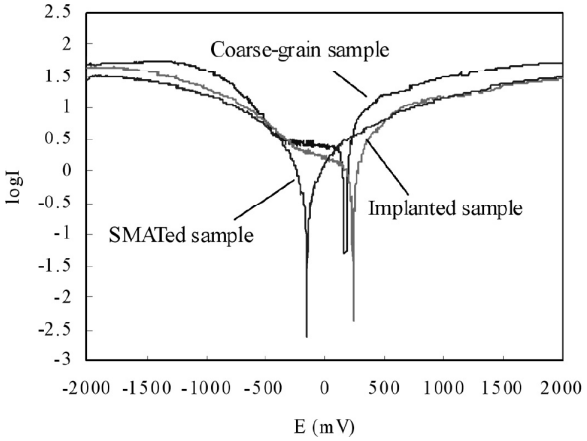

Fig. 6. Polarization curve of the samples.

3.5. Corrosion

The typical anodic polarization curves of Ti implanted samples and SMATed samples are shown in Fig. 6. It is clearly seen that the corrosion behavior of samples was affected by Ti ion implantation. These curves have a qualitatively similar behavior but different electrochemical data values.

In comparison with the coarse-grain copper, the SMATed copper exhibited lower corrosion resistance. The corrosion potential E_{corr} of SMATed copper (E_{corr} =-150 mV) was more negative than that of coarse-grain copper (E_{corr}=174 mV) indicating that the former was easier to passivity than the latter. It is evident that the nanocrystalline copper exhibits a lower activation energy for passivity than that of the coarse-grain copper. The passivity current density I of the nanocrystalline copper was much greater than that of the coarse-grain copper indicating that the nanocrystalline structure enhanced the kinetics of anodic dissolution resulting in a greater dissolution rate for the nanocrystalline copper. The corrosion resistance of materials is dependent upon many factors. For the nanocrystalline metal, it has been demonstrated that its corrosion behavior is greatly affected by reducing the average grain size to the nanocrystalline range. A reduction of grain size results in an enhancement of the activity of the surface atoms and intergranular atoms, giving rise to an increase in passivity ability and, at the same time, an increase in the dissolution rate of the passive film. In addition, the specimen defect caused by the synthesis technique also plays an important role on the corrosion performance of bulk nanocrystalline copper except for grain size. It is impossible to synthesize non-defect nanocrystalline copper bulk using the IGCWC method. Micro-defects such as micro-gap usually occur at the interface between the grains. These areas with defects are corroded preferentially to other areas. Thus the corrosion of nanocrystalline copper is greatly related to these defects that are susceptible to corrosion. In other words, the defects in nanocrystalline materials facilitate the corrosion. In the present case, to a certain extent, the lower resistance of nanocrystalline copper to corrosion is traceable to its defects. These factors mentioned above lead to a decrease in the corrosion resistance of nanocrystalline copper.

Comparing the corrosion potential of the implanted sample and the SMATed sample, an increase of 500 mV was obtained for the implanted sample. The breakdown potential E_{br} corresponding to the onset of pitting corrosion is usually at potential marked by a rapid increase of the passive current density. The maximum of E_{br} of the Ti implanted sample is about 100 mV higher than SMATed samples. The corrosion current density i_{corr} of the samples remarkably decreases after Ti implantation. The minimum of i_{corr} is 9.7×10^{-9} A/cm^2 in samples. The lower i_{corr} means that the Ti implanted samples would be eroded more slowly than the unimplanted sample. Based on the above analysis, it can be concluded that the implantation of titanium in SMATed copper surface leads to the formation of an effective protective passive layer, which possesses better corrosion performance than the coarse-grain copper and the SMATed copper.

4.CONCLUSION

After the surface mechanical attrition treatment (SMAT) the microstructure of the surface layer was refined into the nanoscale. The SMATed copper was modified by Ti implantation. The concentration of implanted ions followed Gauss distribution. The implantation of titanium in SMATed copper surface leads to the formation of an effective protective passive layer, which possesses better corrosion performance than the coarse-grain copper and the SMATed copper.

ACKNOWLEDGEMENTS

The authors gratefully acknowledge the Natural Science Foundation of China (NSFC No.50471070, 50644041), the Nature Science Foundation (2011011020-1) and the Young Subject-Leader Foundation, Shanxi Province, for financial support of this work. Financial support from NCET-04-0257 is also appreciated.

REFERENCES

[1] K. Lu and J. Lu // *J. Mater. Sci. Tech.* **15** (1999) 193.
[2] K. Lu, J.T. Wang and W.D. Wei // *J. Appl. Phys.* **69** (1991) 522.
[3] K. Dai, J. Villegas and Z. Stone // *Acta. Mater.* **52** (2004) 5771.
[4] N.R. Tao, Z.B. Wang and W.P. Tong // *Acta. Mater*. **50** (2002) 4603.
[5] H.W. Zhang, Z.K. Hei and G. Liu // *Acta. Mater.* **51** (2003) 1871.
[6] X.L. Wu, N.R. Tao and Q.M. Wei // *Acta. Mater.* **55** (2007) 5768.
[7] K.Y. Zhu, A. Vassel and F. Brisset // *Acta. Mater.* **52** (2004) 4101.

[8] Y.M. Lin, J. Lu and L.P. Wang // *Acta. Mater.* **54** (2006) 5599.
[9] W. Luo, C. Qian and X.J. Wu // *Mater. Sci. Eng. A*. **452/453** (2007) 524.
[10] Z. He, Z. Wang and W.Wang // *Surf. Coat. Tech.* **201** (2007) 5705
[11] Y.Y. Chang and D.Y. Wang // *Surf .Coat. Tech.* **200** (2005) 2187.
[12] Y. Cheng, C. Wei and K.Y. Gan // *Surf. Coat. Tech.* **176** (2004) 261.
[13] Y.Y. Chang and D.Y. Wang // *Surf. Coat. Tech*. **200** (2005) 2187.
[14] V.I. Safonov, I.G. Marchenko and G.N. Kartmazov // *Surf. Coat. Tech.* **174-175** (2003) 1260.
[15] F.J. Pérez, M.P. Hierro and C. Gómez // *Surf. Coat. Tech.* **155** (2002) 250.
[16] Z.B. Wang, N.R. Tao and W.P. Tong // *Acta. Mater.* **51** (2003) 4319.